BIOCHEMISTRY
including biophysical chemistry & molecular biology

RAPID REPORT

pubs.acs.org/biochemistry

Residue-Specific Fluorescent Probes of α-Synuclein: Detection of Early Events at the N- and C-Termini during Fibril Assembly

Thai Leong Yap, Candace M. Pfefferkorn, and Jennifer C. Lee*

Laboratory of Molecular Biophysics, National Heart, Lung, and Blood Institute, National Institutes of Health, Bethesda, Maryland 20892, United States

Supporting Information

ABSTRACT: In the Parkinson's disease-associated state, α-synuclein undergoes large conformational changes, forming ordered, β-sheet-containing fibrils. To unravel the role of specific residues during the fibril assembly process, we prepared single-Cys mutants in the disordered (G7C and Y136C) and proximal (V26C and L100C) fibril core sites and derivatized them with environmentally sensitive dansyl (Dns) fluorophores. Dns fluorescence exhibits residue specificity in spectroscopic properties as well as kinetic behavior; early kinetic events were revealed by probes located at positions 7 and 136 compared to those at positions 26 and 100.

α-Synuclein (α-syn) is a 140-residue, cytoplasmic, and membrane-associated human protein that is highly expressed in presynaptic nerve terminals.[1] Though it is linked to numerous physiological roles,[2] α-syn is most well-known for its connection to amyloid (fibril) formation[3] and its presence in Lewy bodies, the pathological hallmark of Parkinson's disease.[1] This filamentous material contains ordered β-strands, aligned perpendicular to the fibril axis.[4−7]

Established by various experimental approaches, the α-syn fibril core consists of residues 30−100 with disordered N- and C-terminal regions (Figure 1a).[8−11] While outside the amyloid core, in the soluble state, the N- and C-termini participate in intra- and intermolecular interactions.[12−14] Fluorescence spectroscopy has been effective for studying α-syn conformation [15−18] and aggregation;[19−24] however, kinetic details at the residue level during amyloid formation remain limited. With this in mind, we sought to define residue-specific behaviors of the N-terminus versus C-terminus during protein aggregation by introducing environmentally sensitive dansyl (Dns) [25] fluorescent probes at multiple sites (Figure 1b).

We prepared four single-Cys α-syn mutants in the disordered (G7C and Y136C) and proximal fibril core sites (V26C and L100C) in N- and C-terminal regions and derivatized them with the thiol-reactive Dns precursor, 5-({[(2-iodoacetyl)amino]ethyl}amino)naphthalene-1-sulfonic acid. Minimal Dns protein (1.5%) was used to monitor wild-type (WT) protein aggregation (1.5 μM Dns protein and 100 μM WT). Because α-syn fibril formation generally exhibits sigmoidal kinetics, we took frequent fluorescence and laser light scattering (LS) measurements during the lag, exponential growth, and mature phases (Figure 1c,d).[26−28]

Similar to the WT protein, we find that Dns-labeled proteins are predominantly disordered in solution, adopt helical structure in the presence of sodium dodecyl sulfate micelles,[29] and form β-sheets upon aggregation (Figures S1 and S2 of the Supporting Information).[30] Consistent with the circular dichroism data for the soluble protein, steady-state and excited-state fluorescence properties of the Dns probe were site-independent, reflecting water-exposed fluorophores [mean wavelength $\langle\lambda\rangle$ of ∼525−528 nm (Table S1 of the Supporting Information), average excited state lifetime $\langle\tau\rangle$ of ∼10 ns (data not shown)]. In addition, the morphology of fibrils containing mixtures of WT and Dns-labeled proteins is indistinguishable from that of WT alone (Figure S3 of the Supporting Information). Using the *N*-acetylcysteine derivative of Dns, we ascertained that the fluorophore itself is not a fibril probe (Figure S4 of the Supporting Information). These results show that the Dns-labeled proteins are not measurably different from the WT protein alone and can be used as reporters of α-syn amyloid formation.

Upon aggregation, Dns fluorescence exhibits dramatic spectroscopic and residue-specific sensitivity (Figure 1c and Figure S5 of the Supporting Information). We observe overall intensity increases (1.6−3-fold) and spectral blue shifts ($\Delta\langle\lambda\rangle$ = 16−42 nm) indicating that all Dns sites are sequestered from an aqueous to a more hydrophobic local environment. Unexpectedly, Dns7 and Dns136 ($\Delta\langle\lambda\rangle$ = 42 and 29 nm, respectively), residues outside the amyloid core, were more responsive probes than residues proximal to the core, Dns26 and Dns100 ($\Delta\langle\lambda\rangle$ = 16 and 20 nm, respectively); Dns7 is in the most hydrophobic surrounding, whereas Dns26 and Dns100 appear to be markedly more polar. Anisotropy and fluorescence decay data also show an increased degree of immobilization (Table S1 of the Supporting Information) and lifetimes [$\langle\tau\rangle$ ∼ 12−16 ns (data not shown)].

To assess whether Dns probes are sensitive to early aggregation events,[23,24] we compared kinetics derived from $\langle\lambda\rangle$ to LS measurements that report on macroscopic aggregates (size detection limit of ≥100 nm). From independent experiments, we confirmed that similar midpoint transitions were obtained for LS and the standard thioflavin T (ThT) assay in detecting fibril formation (Figure S6 of the Supporting Information). Because of inherent sample-to-sample variations in the lag phase,[31] during which time small changes in fibril concentration can be detected, we elected to present a full representative data set for the mixture of WT and Dns136 (Figure 1d) to show that despite the uncertainties in the lag times (20−30 h), spectroscopic data ($\langle\lambda\rangle$) and the respective trend [$t_{50}(\Delta\langle\lambda\rangle)$ vs t_{50}(LS), the midpoint transition times] are consistent and reproducible

Received: January 18, 2011
Published: February 21, 2011

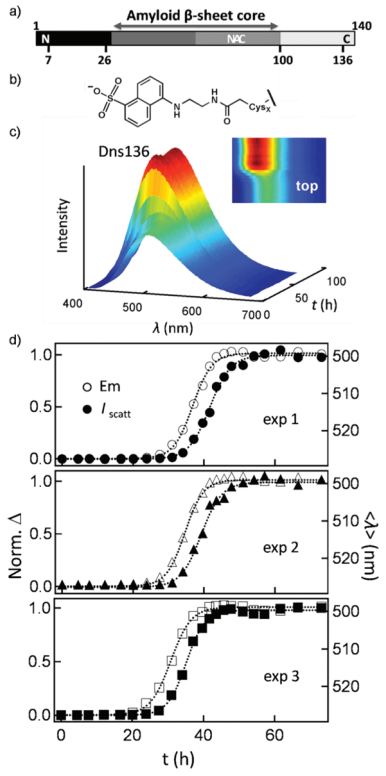

Figure 1. (a) Primary sequence of α-syn highlighting the amyloid β-sheet core (residues 30−100), non-amyloid β component (NAC) region (residues 61−95), and Cys labeling sites (G7C, V26C, L100C, and Y136C) used in this study. (b) Structure of the Dns fluorophore. (c) Representative fluorescence spectra of Dns136 (1.5 μM) during α-syn aggregation (100 μM in 25 mM NaP_i, 100 mM NaCl, pH 7, 37 °C, shaking at 600 rpm, t = 0−75 h). The inset shows the Dns136 emission intensity surface. Dns emission intensity is in arbitrary units (blue to red) normalized to the highest intensity. Data for other sites can be found in Figure S5 of the Supporting Information. (d) Aggregation kinetics for three independent measurements monitored simultaneously by Dns136 emission (Em, empty symbols) and light scattering (I_{scatt}, filled symbols); the typical lag phase is ∼20−30 h. Data for other sites can be found in Figure S7 of the Supporting Information. Left axes represent the normalized change (Norm. Δ) for I_{scatt} and Em, and right axes represent absolute mean wavelength changes ($\langle\lambda\rangle$).

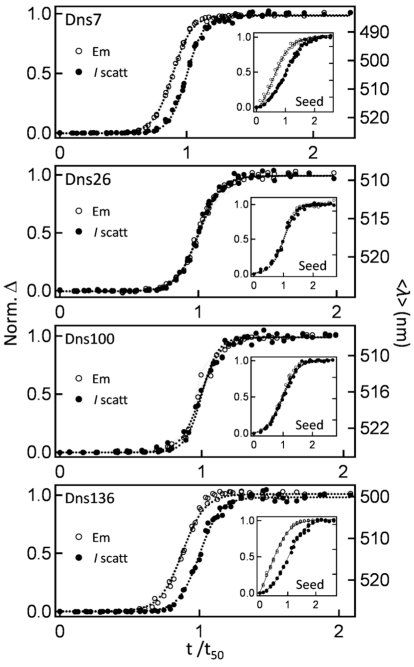

Figure 2. Residue-specific probes of α-syn aggregation in the absence and presence (inset) of preformed seeds (3%). Aggregation kinetics monitored simultaneously by Dns7, -26, -100, and -136 emission [Em (○)] and light scattering [I_{scatt} (●)] for three independent measurements. To compare the different sites, we have normalized the time axes with I_{scatt} midpoint transition times (time it takes to reach 50% of the maximal signal, t_{50}) extracted from fits of respective I_{scatt} data to sigmoidal functions. Left axes represent the normalized change (Norm. Δ), and right axes represent the absolute mean wavelength change ($\langle\lambda\rangle$).

(see Figure S7 of the Supporting Information for other sites). To ascertain that the Dns probe has little effect on WT aggregation kinetics, we performed concentration dependence studies (1.5−9 μM Dns136) and found no apparent differences (Figure S8 of the Supporting Information). We note that while a variety of fluorophores can be chosen for and used to probe α-syn aggregation, larger, more hydrophobic molecules can perturb the kinetics.[21,23,24]

When monitored by Dns fluorescence, both Dns7 and Dns136 exhibit earlier aggregation kinetics compared to Dns26 and Dns100 (Figure S7 of the Supporting Information). Additionally, Dns7- and Dns136-monitored kinetics preceded the LS curves, whereas in contrast, nearly identical behaviors were found for Dns26 and Dns100 compared to that of LS. To quantify the relative residue-specific trend, we used an established analysis method to scale the aggregation time.[32,33] For each set of aggregation data, LS kinetics were fit to sigmoidal functions and the resulting t_{50}(LS) values were used to scale the time axis (t/t_{50}) for all kinetic data ($n \geq 3$) (Figure 2). In accord with the unscaled data, smaller scaled t_{50} (t_{50}^{scaled}) values were observed when monitored by both Dns7 and Dns136 fluorescence [$t_{50}^{scaled}(\Delta\langle\lambda\rangle) = 0.870(3)$] compared to LS values [t_{50}^{scaled}(LS) = 1.000(3) (Table S2 of the Supporting Information)], while probes at positions 26 and 100 fully recapitulate the LS data [$t_{50}^{scaled}(\Delta\langle\lambda\rangle) = 0.990(3) \sim t_{50}^{scaled}$(LS) = 1.000(5)]. Our data suggest that the pathway for amyloid formation for the disordered N- and C-terminal regions develop initially from the ends, followed by residues toward the amyloid core.[34]

The increased sensitivity of the N- and C-terminal distal sites may be coupled to the observation that in solution, these regions are involved in transient interactions.[12−14,35,36] In particular, if the preferred solution configuration is either intraprotein[12,13] (C-to-NAC region, central hydrophobic region that is essential for aggregation) or antiparallel interprotein interaction[14] (N-to-C/C-to-N), then for α-syn to adopt a cross-β fold, where the β-strand residues are suggested to be parallel-in-register (N-to-C/N-to-C),[8,11,37] conformational rearrangement at the N- and C-termini must occur.

To shed light on the specific role of Dns7 and Dns136, we examined if the residue specificity and sensitivity would be retained if we accelerated the lag phase by seeding with 3% WT fibrils (see the Supporting Information for experimental details). Because α-syn aggregation kinetics can be described as a nucleation and nucleation-dependent elongation mechanism,[26−28] the observed early transition could reflect formation of intermediates or oligomers as well as initial filament elongation processes. Upon seeding, the lag phase will be significantly

reduced and sometimes even abolished;[38] thus, if the detected early events are related to nucleation, the observed differences between $t_{50}(\Delta\langle\lambda\rangle)$ and $t_{50}(\mathrm{LS})$ should diminish.

Consistent with spontaneous aggregation, the seeded samples showed earlier transitions for residues 7 and 136 [$t_{50}{}^{\mathrm{scaled}}(\Delta\langle\lambda\rangle) = 0.58(6)$ and $0.39(3)$, respectively;[39] $t_{50}{}^{\mathrm{scaled}}(\mathrm{LS}) = 1.00(1)$ (Figure 2, inset, and Table S2 of the Supporting Information)]. However, when monitored by Dns26 and Dns100, both showed identical fluorescence and LS kinetics data. Accordingly, we propose that these early conformational rearrangements likely occur after nucleation and represent filament formation or elongation processes.

In summary, our study has provided site-specific information about the role of the α-syn N- and C-termini in amyloid formation. Kinetics obtained for Dns fluorophores in the disordered (7 and 136) regions precede proximal (26 and 100) amyloid core sites. Both seeded and spontaneous aggregation kinetics suggest that residues 7 and 136 exhibit local conformational and environmental changes prior to, whereas changes for residues 26 and 100 occur concomitantly with, macroscopic fibril formation. Our results support the hypothesis that local structural reorganization at the N- and C-termini is necessary for α-syn to break the conformational constraints from either intra- or interpolypeptide electrostatic attraction and, thus, favors the formation of parallel, in-register, β-sheet fibrils.

■ ASSOCIATED CONTENT

Supporting Information. Supplementary figures, tables, and detailed experimental methods. This material is available free of charge via the Internet at http://pubs.acs.org.

■ AUTHOR INFORMATION

Corresponding Author

*E-mail: leej4@mail.nih.gov. Telephone: (301) 496-3741. Fax: (301) 402-3404.

Funding Sources

Supported by the Intramural Research Program of the National Heart, Lung, and Blood Institute, National Institutes of Health.

■ ACKNOWLEDGMENT

We thank Mathew Daniels and Patricia Connelly (EM Core Facility), Greg Piszczek (Biophysics Facility), and Duck-Yeon Lee (Biochemistry Core) for technical assistance and Julie Maylor for synthesizing the Dns model complex.

■ REFERENCES

(1) Cookson, M. R. (2005) *Annu. Rev. Biochem. 74*, 29–52.
(2) Uversky, V. N., and Eliezer, D. (2009) *Curr. Protein Pept. Sci. 10*, 483–499.
(3) Seshadri, S., Oberg, K. A., and Uversky, V. N. (2009) *Curr. Protein Pept. Sci. 10*, 456–463.
(4) Margittai, M., and Langen, R. (2008) *Q. Rev. Biophys. 41*, 265–297.
(5) Tompa, P. (2009) *FEBS J. 276*, 5406–5415.
(6) Tycko, R. (2006) *Q. Rev. Biophys. 39*, 1–55.
(7) Serpell, L. C., Berriman, J., Jakes, R., Goedert, M., and Crowther, R. A. (2000) *Proc. Natl. Acad. Sci. U.S.A. 97*, 4897–4902.
(8) Chen, M., Margittai, M., Chen, J., and Langen, R. (2007) *J. Biol. Chem. 282*, 24970–24979.
(9) Heise, H., Hoyer, W., Becker, S., Andronesi, O. C., Riedel, D., and Baldus, M. (2005) *Proc. Natl. Acad. Sci. U.S.A. 102*, 15871–15876.
(10) Qin, Z., Hu, D., Han, S., Hong, D. P., and Fink, A. L. (2007) *Biochemistry 46*, 13322–13330.
(11) Vilar, M., Chou, H. T., Luhrs, T., Maji, S. K., Riek-Loher, D., Verel, R., Manning, G., Stahlberg, H., and Riek, R. (2008) *Proc. Natl. Acad. Sci. U.S.A. 105*, 8637–8642.
(12) Bertoncini, C. W., Jung, Y. S., Fernandez, C. O., Hoyer, W., Griesinger, C., Jovin, T. M., and Zweckstetter, M. (2005) *Proc. Natl. Acad. Sci. U.S.A. 102*, 1430–1435.
(13) Hoyer, W., Cherny, D., Subramaniam, V., and Jovin, T. M. (2004) *Biochemistry 43*, 16233–16242.
(14) Wu, K. P., and Baum, J. (2010) *J. Am. Chem. Soc. 132*, 5546–5547.
(15) Lee, J. C., Langen, R., Hummel, P. A., Gray, H. B., and Winkler, J. R. (2004) *Proc. Natl. Acad. Sci. U.S.A. 101*, 16466–16471.
(16) Pfefferkorn, C. M., and Lee, J. C. (2010) *J. Phys. Chem. B 114*, 4615–4622.
(17) Trexler, A. J., and Rhoades, E. (2009) *Biochemistry 48*, 2304–2306.
(18) Ferreon, A. C. M., Moran, C. R., Ferreon, J. C., and Deniz, A. A. (2010) *Angew. Chem. 49*, 3469–3472.
(19) Dusa, A., Kaylor, J., Edridge, S., Bodner, N., Hong, D. P., and Fink, A. L. (2006) *Biochemistry 45*, 2752–2760.
(20) Kaylor, J., Bodner, N., Edridge, S., Yamin, G., Hong, D. P., and Fink, A. L. (2005) *J. Mol. Biol. 353*, 357–372.
(21) Thirunavukkuarasu, S., Jares-Erijman, E. A., and Jovin, T. M. (2008) *J. Mol. Biol. 378*, 1064–1073.
(22) van Rooijen, B. D., van Leijenhorst-Groener, K. A., Claessens, M. M. A. E., and Subramaniam, V. (2009) *J. Mol. Biol. 394*, 826–833.
(23) Yushchenko, D. A., Fauerbach, J. A., Thirunavukkuarasu, S., Jares-Erijman, E. A., and Jovin, T. M. (2010) *J. Am. Chem. Soc. 132*, 7860–7861.
(24) Nath, S., Meuvis, J., Hendrix, J., Carl, S. A., and Engelborghs, Y. (2010) *Biophys. J. 98*, 1302–1311.
(25) Lakowicz, J. R. (2006) *Principles of fluorescence spectroscopy*, 3rd ed., Springer, New York.
(26) Morris, A. M., Watzky, M. A., and Finke, R. G. (2009) *Biochim. Biophys. Acta 1794*, 375–397.
(27) Harper, J. D., and Lansbury, P. T., Jr. (1997) *Annu. Rev. Biochem. 66*, 385–407.
(28) Wood, S. J., Wypych, J., Steavenson, S., Louis, J. C., Citron, M., and Biere, A. L. (1999) *J. Biol. Chem. 274*, 19509–19512.
(29) Ulmer, T. S., Bax, A., Cole, N. B., and Nussbaum, R. L. (2005) *J. Biol. Chem. 280*, 9595–9603.
(30) We estimate the aggregation yield to be 80−90%, as assessed by UV spectroscopic analysis of the remaining soluble protein. While the absolute amount of β-sheet-containing fibrils is difficult to determine, we find comparable CD spectroscopic signals (217−218 nm) as in previous work.[21]
(31) Xue, W. F., Homans, S. W., and Radford, S. E. (2008) *Proc. Natl. Acad. Sci. U.S.A. 105*, 8926–8931.
(32) Larson, J. L., and Miranker, A. D. (2004) *J. Mol. Biol. 335*, 221–231.
(33) Shim, S. H., Gupta, R., Ling, Y. L., Strasfeld, D. B., Raleigh, D. P., and Zanni, M. T. (2009) *Proc. Natl. Acad. Sci. U.S.A. 106*, 6614–6619.
(34) Using similar analysis of the human islet amyloid polypeptide implicated in type 2 diabetes, the inner core residues exhibited the earliest transitions while changes at residues on the N- and C-termini occurred later.[33]
(35) Lee, J. C., Gray, H. B., and Winkler, J. R. (2005) *J. Am. Chem. Soc. 127*, 16388–16389.
(36) Allison, J. R., Varnai, P., Dobson, C. M., and Vendruscolo, M. (2009) *J. Am. Chem. Soc. 131*, 18314–18326.
(37) Der-Sarkissian, A., Jao, C. C., Chen, J., and Langen, R. (2003) *J. Biol. Chem. 278*, 37530–37535.
(38) Yagi, H., Kusaka, E., Hongo, K., Mizobata, T., and Kawata, Y. (2005) *J. Biol. Chem. 280*, 38609–38616.
(39) The variations between seeded and spontaneous $t_{50}{}^{\mathrm{scaled}}(\Delta\langle\lambda\rangle)$ obtained for Dns7 and Dns136 likely reflect the number and quality of the seeds introduced, which are difficult to control. For example, when the WT protein was seeded with 5% WT seed, we measured a $t_{50}{}^{\mathrm{scaled}}(\Delta\langle\lambda\rangle)$ of 0.45(2) for Dns7.